Numerical study of balcony deformations taking into account the presence of thermal break system.

Tuan-Anh NGUYEN [1, 2, *], Piseth HENG [1, 3], Hugues SOMJA [1], Quang-Huy NGUYEN [1]

1. Structural Engineering Research Group, INSA de Rennes, Rennes, France
2. Section of Structural Engineering, University of Transport and Communications, Hanoi, Vietnam
3. INGENOVA, Civil Engineering Office, 5 rue Louis Jacques Daguerre, Saint-Jacques-de-la-Lande, France

[*]Corresponding author email: tuananh_ktxd@utc.edu.vn

Abstract

This paper deals with the development of a numerical model for predicting the behaviour of the balcony in buildings equipped with internal insulation and thermal break systems while taking into account the torsional stiffness of the lintel and other restraints. In fact, the equipment of thermal break systems can help to limit the problem of thermal bridge formed through structural components of balcony-floor junction. However the balcony deflections become important comparing to the non-equipped case. The latter is computed in common practices by considering the balcony-floor structure as continuous beams, submitted to only bending-flexural effect. In some cases, the lintel can be used as an intermediary element to reduce the deflection of the balcony. This horizontal reinforced concrete (RC) beam is submitted to a combined loading of flexion and torsion, which requires specific numerical model to resolve.

In the proposed numerical modelling, the balcony-lintel-floor structure is represented by a beam grid model, in which the floor and balcony are divided into several bands perpendicular to the lintel. The lintel, considered as the main problem, is modelled using the finite element multi-fiber approach and the displacement-based formulation, which are capable of predicting the flexural and torsional behaviour of RC members. The same type of model with fewer degrees of freedom is also used to determine the flexural behaviours of the floor and that of the balcony. The thermal break behaviours are represented by a pair of rotational and axial springs in order to transmit the shear force and bending moment from the floor to the lintel. Another system of springs are also used to reproduce the axial and bending stiffness of the walls. While the efforts issued from the balcony and the walls can be determined explicitly, the presence of thermal break requires an iterative process to compute the displacement and rotation of the lintel.

Keywords: *Multi-fiber finite element; Thermal break systems; Thermal bridges; Combined torsional and flexural behaviours.*

1. Introduction

In buildings with internal and/or external insulation, thermal bridges occur at the connections between structural elements such as the balcony, walls and floor. These discontinuities of insulation provoke energy losses, increase the risk of local condensation and reduce the effectiveness of insulation. The presence of thermal bridges can be avoided with the equipment of thermal break systems, an element of low thermal conductivity placed at the building junctions to reduce the flow of thermal energy between structural components. Many types of thermal break systems are provided and suggested for different structural connections (wall-floor, balcony-wall-floor) and material designs (concrete-concrete, concrete-steel or concrete-timber structures) (Ancon® 2018, COHB Industrie® 2019, Schöck Isokorb® 2018).

For building with internal insulation, in the case of balcony connectors, the presence of thermal break system might however increase the balcony deflections comparing to the non-equipped case (Figure 1-a). In common practice, the latter is computed by considering the balcony-floor structures as continuous

beams, submitted to only bending-flexural effect. In some common cases, especially with wall openings, the lintel can be used as an intermediary element to reduce the deflection of the balcony (Figure 1-b). This horizontal reinforced concrete (RC) beam is submitted to a combined loading of flexion and torsion, which requires specific numerical model to resolve. The balcony deformations therefore cannot be computed according to the common practice way and requires an improved method.

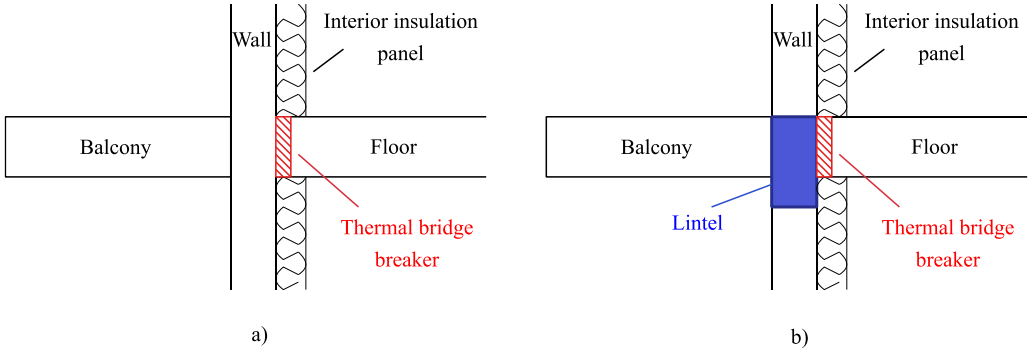

Figure 1. The presence of thermal break in the case of balcony connector.

In the proposed numerical modelling, the balcony-lintel-floor structure is represented by a beam grid model, in which the floor and balcony are divided into several bands perpendicular to the lintel. In other words, the complex three-dimensional structure is modelled using a simpler system of beam elements, in which the lintel is considered as the main element. The bending moment issued from the balcony and the floor creates a torsional effect in the lintel, which is modelled using the finite element multi-fiber approach and the displacement-based formulation. This approach has been widely used to correctly predict the flexural and torsional behaviour of RC members (Bairan and Mari 2007, Navarro et al. 2007, Nguyen, Nguyen and Somja 2019). The same type of model with fewer degrees of freedom is also used to determine the flexural behaviours of the floor and that of the balcony.

The shear force and bending moment are transmitted from the floor to the lintel through the thermal break system, whose behaviours are represented by a pair of rotational and axial springs of elastic and/or elasto-plastic stiffness. Another system of springs are also used to reproduce the axial and bending stiffness of the walls. While the efforts issued from the balcony and the walls can be determined explicitly, the presence of thermal break requires an iterative process to compute the displacement and rotation of the lintel. These displacements are then defined as the boundary conditions to calculate the balcony deflections. The numerical results obtained by the proposed model are compared and evaluated with a solid finite element model simulated on ABAQUS software.

2. Model description

The proposed model has been developed with the intention to study the structure of balcony-lintel-walls-floor-thermal break (Figure 2), for which the structural dimensions and parameters are shown in Table 1.

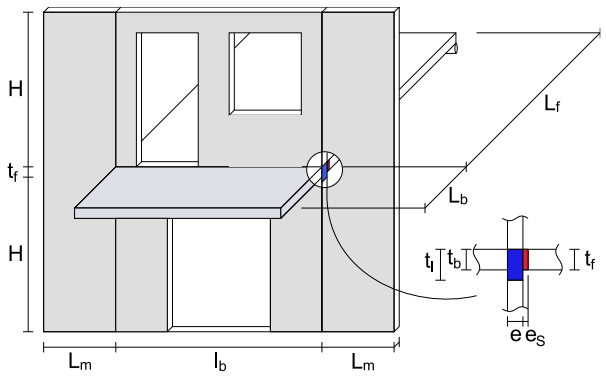

Figure 2. General structure of balcony-lintel-walls-floor-thermal break.

Table 1. The parameters of studied structure.

Balcony	Walls	Lintel	Floor	Thermal break
Length L_b Width l_b Thickness t_b	Height H Thickness e Mullions width L_m Wall openings	Height t_l Width e (= the wall thickness)	Length L_f Thickness t_f	Width Thickness e_s

According to the introduction, the structural components are modelled by two different ways:

- The balcony, lintel and floor: a beam grid-type model in which the floor and balcony are divided into several bands perpendicular to the lintel (Figure 3). Each band of beam is modelled by a multi-fiber finite element approach.

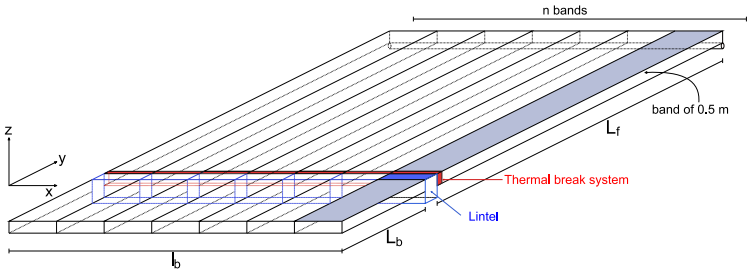

Figure 3. Beam grid model for the balcony-lintel-floor system.

- The walls and the thermal break system: a pair of rotational and axial springs of elastic and/or elasto-plastic stiffness (Figure 4). The bending and axial effect of the wall are zero in the wall opening positions, therefore no spring is modelled.

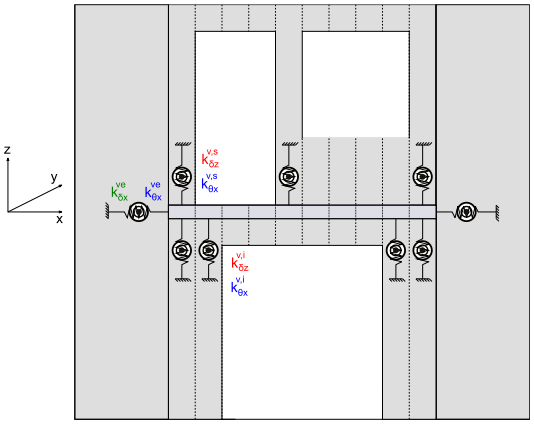

Figure 4. Pair of springs modelling the walls and thermal break system effect.

Being the main problem, the lintel is subjected to a combined loading of shear forces and torsional moments coming from the balcony and the thermal break – floor combination, as well as from the walls. While the efforts from the balcony can be computed explicitly, the determination of the external efforts coming from the floor is not evident due to the presence of the thermal break. An iterative procedure is thus necessary in order to determine these efforts and then the sectional deformations of the lintel. The calculation procedure is summarized in Figure 5 and includes 3 steps:

1. Estimate the initial deflection $v_z^{l.0}$ and rotation $\theta_x^{l.0}$ of the lintel in each band of beam. The numerical model for this step is called Lintel Model 1.

2. At the first iteration, taking $v_z^{l,k=1} = v_z^{l,0}$ and $\theta_x^{l,k=1} = \theta_x^{l,0}$ .Then, using theses lintel deformations as the boundary conditions, the values of shear force $V_z^{S.k}$ and bending moment $M_x^{S.k}$ retained from the thermal break – floor system to the lintel are determined in each band of beam using the second numerical model called Slab Model.

3. Applying the efforts $V_z^{S.k}$ and $M_x^{S.k}$ obtained from previous step to the third numerical model (called Lintel Model 2), the new lintel deformations $v_z^{l.k+1}$ and $\theta_x^{l.k+1}$ can be determined in each band of beam. The Lintel Model 2 is very similar to the first one, except that the effect coming from the thermal break – floor system (shear force V_z^S and spring stiffness $k_{\theta x}^S$) is replaced by a couple of torsional moment and shear force.

The convergence criterion is determined by calculating the relative error of lintel deformations:

$$\varepsilon_v = \frac{v_z^{l,k+1} - v_z^{l,k}}{v_z^{l,k}}; \varepsilon_\theta = \frac{\theta_x^{l,k+1} - \theta_x^{l,k}}{\theta_x^{l,k}} \quad (1.1)$$

- If $\varepsilon_v \le \varepsilon_v^{tol}$ and $\varepsilon_\theta \le \varepsilon_\theta^{tol}$, the iteration process is done; $\varepsilon_v^{tol}, \varepsilon_\theta^{tol}$ are the tolerance limits.
- If not, back to step 2 and taking $v_z^{l,k} = v_z^{l,k-1}$ and $\theta_x^{l,k} = \theta_x^{l,k-1}$.

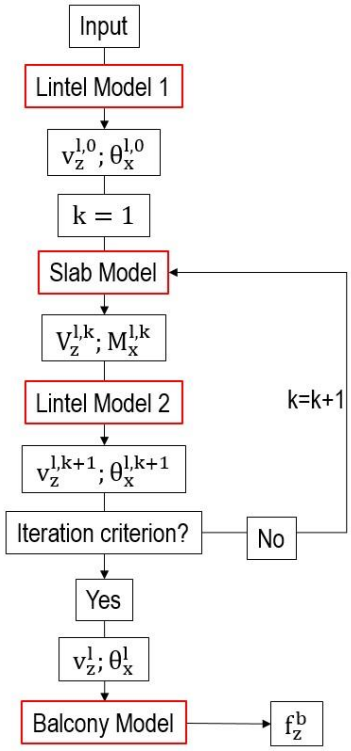

Figure 5. Summarize of the proposed model.

3. Model formulations

3.1. Lintel Models

According to the model description, the proposed model contains two types of Lintel Model: the first one is used in the 1st step and the second one is used in the 3rd step. The only difference between these two types is the applied efforts issue from the thermal break – floor system. The Lintel Models are developed using a two-node Timoshenko beam based on the principle of multi-fiber finite element approach, in which a system of integration points (called fiber) is obtained at the intersection of the longitudinal fibers and some control cross-sections along the element (Figure 6). Each fiber is considered as a material point, has its own coordinates, surface and an appropriate material law in order to determine the strain and stress from the element displacements. Using displacement-based formulation, the internal and nodal efforts, as well as the stiffness matrices, are determined from the generalized and nodal displacements with the aid of numerical integrations and the Gauss-Lobatto interpolation method.

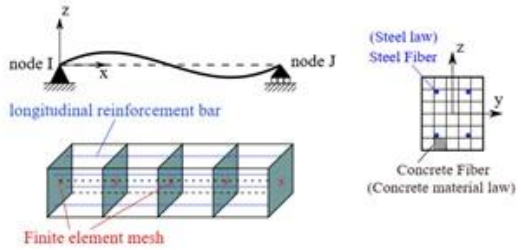

Figure 6. Principle of multi-fiber finite element modelling and section discretization of Lintel Models.

The Lintel Models contain the entire beam of lintel and eventually the mullions at two ends. These beam models are then divided into several elements whose number is defined according to the band of beam (Figure 7). Taking into account the combination of bending and torsional moments, the Lintel Models have 6 degrees of freedom at each element node, resulting a 12x12 stiffness matrix in each element.

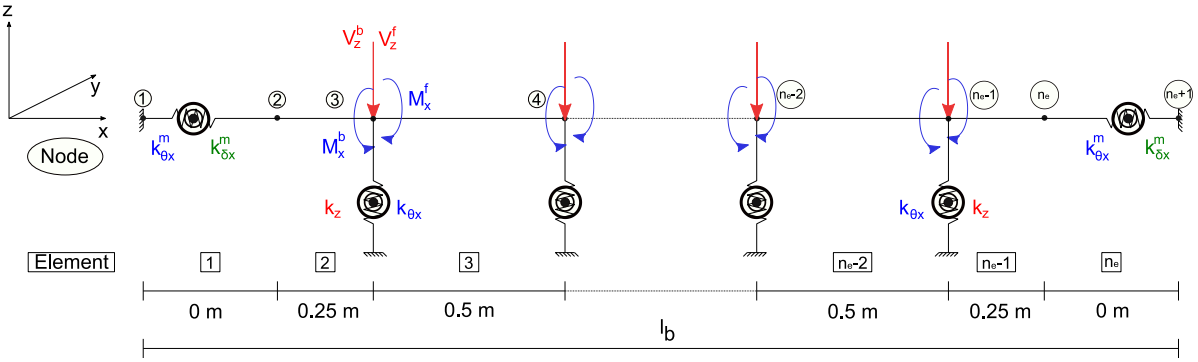

Figure 7. Finite element modelling of lintel.

Each band of lintel is subjected to the external effects from the balcony, walls, mullions and thermal break – floor system. In the 1st step the thermal break effect is not taken into account, and a spring with rotational stiffness is used to represent the bending moment effect from the floor applied in the Lintel Model 1 (Figure 8).

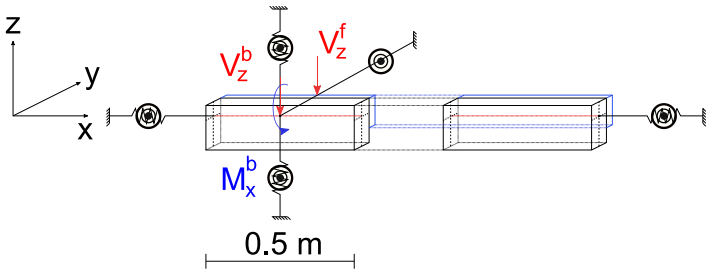

Figure 8. Applied efforts and additional springs in the Lintel Model 1.

In step 3, the effects from thermal break – floor system applied to the lintel are represented by a couple of shear force V_z^S and torsional moment M_x^S, obtained from step 2 (Figure 9).

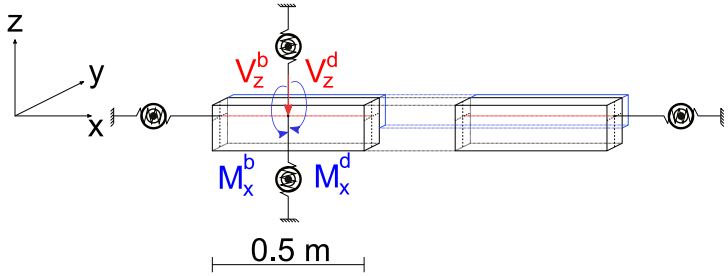

Figure 9. Applied efforts and additional springs in the Lintel Model 2.

The effects of the springs, which are used to model the effects of the walls, mullions and eventually the floor, add some complementary elements into the existing element stiffness matrices of the lintel beam:

$$K_e^{proposed} = K_e^{lintel} + \begin{bmatrix} 0 & 0 & 0 & 0 & 0 & 0 & 0 & 0 & 0 & 0 & 0 & 0 \\ 0 & 0 & 0 & 0 & 0 & 0 & 0 & 0 & 0 & 0 & 0 & 0 \\ 0 & 0 & k_x^m + k_z^w & 0 & 0 & 0 & 0 & 0 & 0 & 0 & 0 & 0 \\ 0 & 0 & 0 & k_{\theta x}^m + k_{\theta x}^w + k_{\theta x}^f & 0 & 0 & 0 & 0 & 0 & 0 & 0 & 0 \\ 0 & 0 & 0 & 0 & k_{\theta y}^m + k_{\theta y}^w & 0 & 0 & 0 & 0 & 0 & 0 & 0 \\ 0 & 0 & 0 & 0 & 0 & 0 & 0 & 0 & 0 & 0 & 0 & 0 \\ 0 & 0 & 0 & 0 & 0 & 0 & 0 & 0 & 0 & 0 & 0 & 0 \\ 0 & 0 & 0 & 0 & 0 & 0 & 0 & 0 & 0 & 0 & 0 & 0 \\ 0 & 0 & 0 & 0 & 0 & 0 & 0 & 0 & k_x^m + k_z^w & 0 & 0 & 0 \\ 0 & 0 & 0 & 0 & 0 & 0 & 0 & 0 & 0 & k_{\theta x}^m + k_{\theta x}^w + k_{\theta x}^f & 0 & 0 \\ 0 & 0 & 0 & 0 & 0 & 0 & 0 & 0 & 0 & 0 & k_{\theta y}^m + k_{\theta y}^w & 0 \\ 0 & 0 & 0 & 0 & 0 & 0 & 0 & 0 & 0 & 0 & 0 & 0 \end{bmatrix} \quad (1.2)$$

The superscripts m, w and f indicate mullion, wall and floor, respectively. The values of theses complementary stiffness are defined as follows (Table 2):

Table 2. Spring stiffness.

Mullions	Walls	Floor
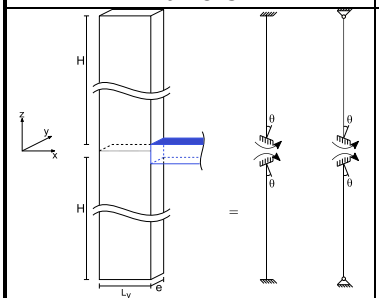	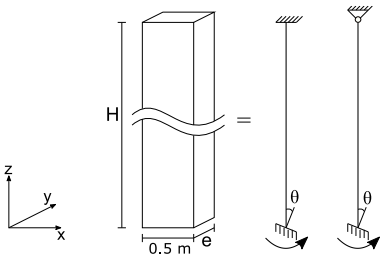	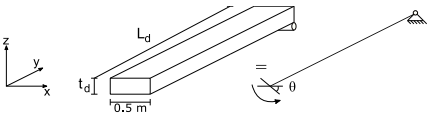
$k_z^m = \frac{E_c^m A}{H}$ $k_{\theta x}^m = 3\frac{E_c^m I_x^m}{H}$ (pinned) $k_{\theta y}^m = 3\frac{E_c^m I_y^m}{H}$ (pinned)	$k_z^w = \frac{E_c^w A}{H}$ $k_{\theta x}^w = 3\frac{E_c^w I_x^w}{H}$ (pinned) $k_{\theta y}^w = 3\frac{E_c^w I_y^w}{H}$ (pinned)	$k_{\theta x}^f = 3\frac{E_c^f I_x^f}{L_f}$

3.2. Slab and Balcony Models

According to the model description, the Slab Model is used in step 2 to represent the behaviour of thermal break – floor system. By defining the lintel displacements obtained from step 1 as the boundary conditions, this model determines the values of shear force $V_z^{S.k}$ and bending moment $M_x^{S.k}$ retained from the thermal break – floor system to the lintel (Figure 10). At the end of the iteration process, at each band of beam, the lintel displacements are defined as the boundary conditions in the Balcony Model to determine the balcony deflections (Figure 5 and 11).

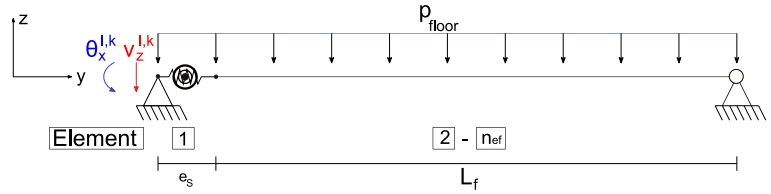

Figure 10. Slab Model - plan view xy.

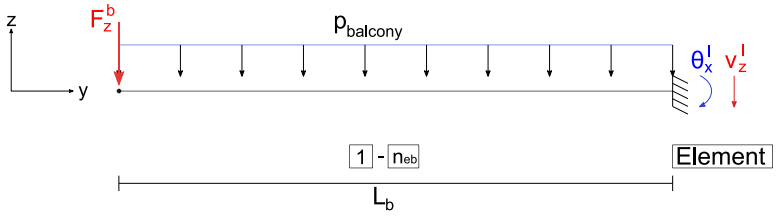

Figure 11. Balcony Models.

Each band of the floor as well as the balcony are modelled on the same principle using a two-node Timoshenko beam based on the multi-fiber finite element approach and displacement-based formulation, similar to the Lintel Models. However, knowing that this type of model is used to represent the behaviour of the thermal break – floor system and the balcony, which are subjected to bending flexural effects, only 3 degrees of freedom are necessary at each element node. This is the reason why in each cross-section layer discretization is applied, instead of square fiber discretization. The beam formulations of these models are similar to those of the Lintel Models with only a few differences in the kinematic equilibrium.

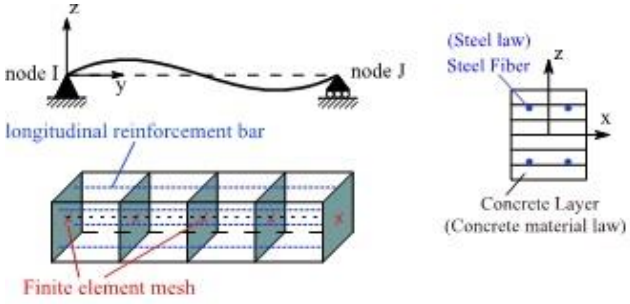

Figure 12. Principle of multi-fiber finite element modelling and section discretization of Slab and Balcony Models.

On the other hand, the thermal break is modelled by a pair of axial and rotational springs with elastic or elasto-plastic stiffness. Knowing that the multi-fiber model of the floor contains 3 degrees of freedom in each element node, the element stiffness matrix of this element is expressed as follows:

$$K_{elastic}^{t-b} = \begin{bmatrix} 0 & 0 & 0 & 0 & 0 & 0 \\ 0 & k_z^{TB} & 0 & 0 & -k_z^{TB} & 0 \\ 0 & 0 & k_{\theta x}^{TB} & 0 & 0 & k_{\theta x}^{TB} \\ 0 & 0 & 0 & 0 & 0 & 0 \\ 0 & -k_{\delta z}^{TB} & 0 & 0 & k_z^{TB} & 0 \\ 0 & 0 & k_{\theta x}^{TB} & 0 & 0 & k_{\theta x}^{TB} \end{bmatrix} \quad K_{e-p}^{t-b} = \begin{bmatrix} 0 & 0 & 0 & 0 & 0 & 0 \\ 0 & k_{11}^{TB} & k_{12}^{TB} & 0 & -k_{11}^{TB} & k_{12}^{TB} \\ 0 & k_{21}^{TB} & k_{22}^{TB} & 0 & -k_{21}^{TB} & k_{22}^{TB} \\ 0 & 0 & 0 & 0 & 0 & 0 \\ 0 & -k_{11}^{TB} & -k_{12}^{TB} & 0 & k_{11}^{TB} & -k_{12}^{TB} \\ 0 & k_{21}^{TB} & k_{22}^{TB} & 0 & -k_{21}^{TB} & k_{22}^{TB} \end{bmatrix} \quad (1.3)$$

Where k_z^{TB},$k_{\theta x}^{TB}$ are the axial and rotational elastic resistance of the thermal break, respectively, while k_{11}^{TB},k_{12}^{TB},k_{21}^{TB},k_{22}^{TB} are the components of the elasto-plastic stiffness matrix.

4. Numerical results

In this section, several numerical examples are carried out for a structure in real condition containing the elements of balcony – lintel – walls – floor and the thermal break SLABE BZ (COHB Industrie® 2019), manufactured by COHB Industry, France. The dimensions of structural elements are represented in Figure 13, in which several balcony widths varied from 2 m to 12 m are considered. Only the case of no wall openings is considered in this paper. The numerical results are obtained by the proposed model in the elastic domain and then compared to a solid finite element model simulated on Abaqus, in which the thermal break system is simulated by the Spring/Dashpots option. The value of elastic modulus is rounded to 10e3 MPa in order to take into account the effect of creep and crack in concrete. In Eurocode 2, under the serviceability limit state and taking into account a value of 0.3 for the Ψ factor, the quasi-permanent combination of actions on the balcony and on the floor are 7.05 kN/m and 6 kN/m, respectively. It is important to note that the value of variable action Q_f is not considered in order to obtain the most unfavourable value of balcony deflection.

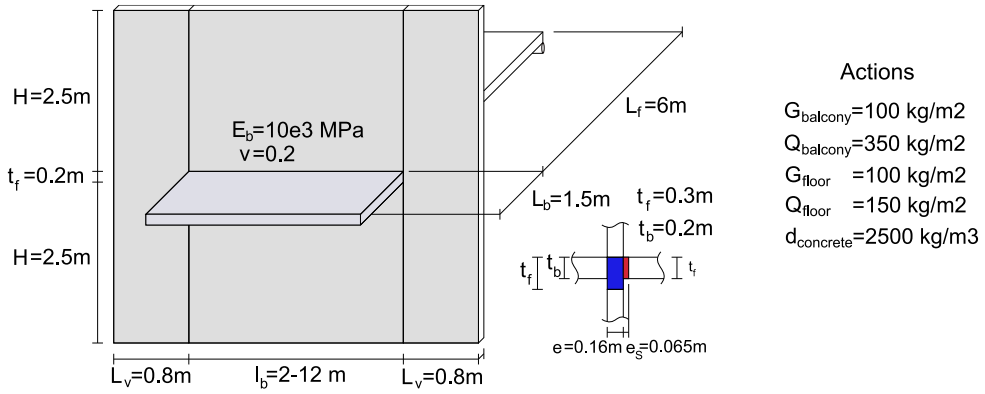

Figure 13. Dimension of studied structure.

4.1. Thermal break and lintel effect

In the case without the presence of thermal break and lintel (configuration 1), the common practice method uses a beam element to represent the behaviour of studied structure, in which the balcony has a positive deflection upward (Figure 14).

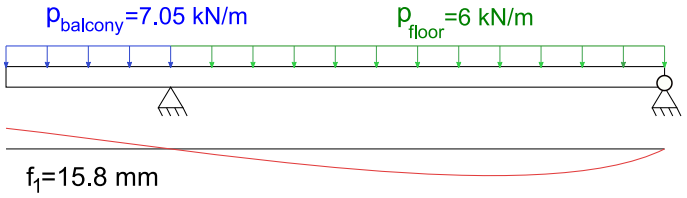

Figure 14. Configuration 1 - Without the presence of thermal break and lintel.

While the thermal break system is taken into account (configuration 2), the common practice method gives a negative deflection downward, whose value is very important and exceeds the limit state of deflection (Figure 15).

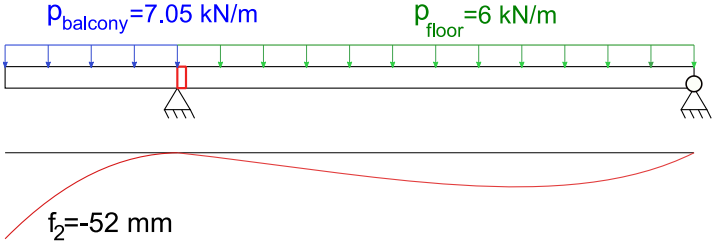

Figure 15. Configuration 2 - Without the presence of lintel.

The common practice method, however, cannot consider the lintel effect on the moment transmission between the floor and the balcony: part of negative moment coming from the thermal break – floor system is resisted by the lintel, due to its capacity of torsional resistance (Figure 17).

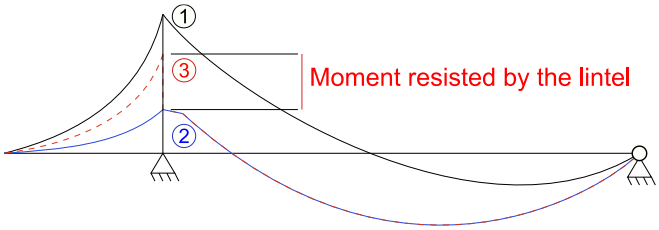

Figure 17. Torsional moment resisted by the lintel.

As a consequence, using the proposed method, the value of balcony deflection reduces from 52 mm according to common practice method to 1 mm, thus satisfying the limit state of deflection (Figure 18).

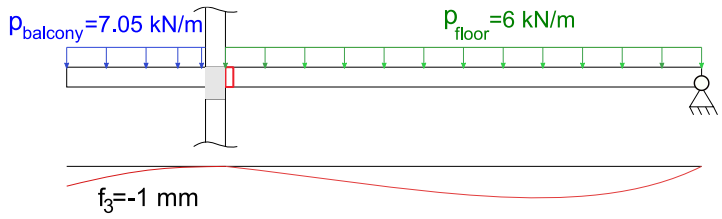

Figure 18. Configuration 3 - With the presence of thermal break and lintel.

4.2. Structure behaviour

In accordance to the practice requirement, the structure behaviour is studied in function of the balcony width. The numerical results are presented in Table 3, for both case of solid model ABAQUS and proposed model, in which only the maximum values at the central band are represented. We can observe that the values of lintel displacements and balcony deflection vary with the balcony width, and reasonable agreements are obtained in most cases effects. As the grid-beam model is in fact more a "band" model, it does not take into account the effect of bending and stress distribution in the transversal direction in the slab and in the walls, and therefore its deflections are bigger than the one obtained with ABAQUS.

Table 3. Numerical results obtained by proposed model and solid model ABAQUS.

	Lintel deflection (e-6 m)		Lintel rotation (e-4 rad)		Balcony deflection (e-3 m)	
Balcony width (m)	Solid model ABAQUS	Proposed model	Solid model ABAQUS	Proposed model	Solid model ABAQUS	Proposed model
2	-24.00	-21.83	1.71	2.20	-1.02	-1.04
3	-24.00	-22.52	2.01	2.45	-1.06	-1.08
6	-24.00	-22.46	2.38	2.58	-1.12	-1.10
12	-23.90	-22.47	2.49	2.58	-1.15	-1.10

The relative differences of numerical results between two models decrease with increasing the balcony width. The distributions of balcony deflection across its width are shown in Figure 19, in which the solid model ABQUS always gives a parabolic shape for every balcony width. On the other hand, for short balcony widths (2 and 3 m), the balcony deflection distributions also have a parabolic shape, but become nearby constant in the middle for large balcony width (6 and 12 m). The variation trend of the balcony deflections in function of its width is also represented in Figure 20, in which the maximum value of balcony deflection obtained by proposed model tends to reach a constant value by increasing the balcony width.

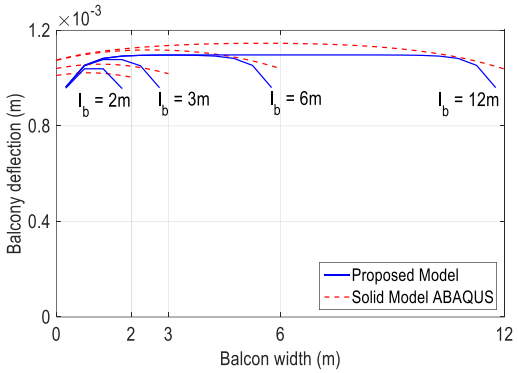

Figure 19. Distribution of balcony deflection across its width.

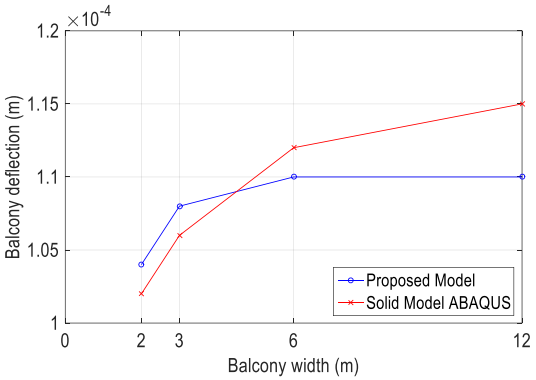

Figure 20. Variation trend of maximum balcony deflection in function of its width.

5. Conclusion

This paper introduces a beam grid model modelling the building behaviour in the presence of thermal break system. The proposed model is simple but effective in predicting the balcony deflection taking into account the torsional resistance capacity of the lintel, which cannot be computed using common practice methods. Good agreements on the numerical results compared to a solid finite element model simulated on ABAQUS prove the accuracy of the proposed model on the elastic linear range. Further studies on the inelastic range will be carried out in order to evaluate the application of this model in practical conditions.

References

Ancon® (2018). Isotec Thermally Insulated Balcony Connectors - Proceedings of the 2017 fib Symposium, Maastricht, The Netherlands, 24-32.

Bairan, J., Mari, A. (2007). Multiaxial-coupled analysis of RC cross-sections subjected to combined forces. Engineering Structures, 29, 1722-1738.

COHB Industrie® (2019). SLABE Boîtier isolant structurel - Avis Technique 3.1/16-368_V1.

Navarro-Gregori, J., Miguel, P., Fernandez, M. & Filippou, F. (2007). A 3d numerical model for reinforced and prestressed concrete elements subjected to combined axial, bending, shear and torsion loading. Engineering Structures, 29, 3404-3419.

Nguyen, T-A., Nguyen, Q-H., Somja, H.. (2019). An enhanced finite element model for reinforced concrete members under torsion with consistent material parameters. Finite Element in Analysis and Design, 167.

Schöck Isokorb® (2018). Thermal bridging solutions with Schöck Isokorb® - Brochure.